



Static and dynamic tensile failure characteristics of rock based on splitting test of circular ring

Di-yuan LI¹, Tao WANG¹, Teng-jiao CHENG², Xiao-lei SUN¹

1. School of Resources and Safety Engineering, Central South University, Changsha 410083, China;

2. China Nerin Engineering Co., Ltd., Nanchang 330031, China

Received 14 January 2016; accepted 6 June 2016

Abstract: Static and dynamic splitting tests were conducted on ring marble specimens with different internal diameters to study the tensile strength and failure modes with the change of the ratio of internal radius to external radius (ρ) under different loading rates. The results show that the dynamic tensile strength of disc rock specimen is approximately five times its static tensile strength. The failure modes of ring specimens are related to the dimension of the internal hole and loading rate. Under static loading tests, when the ratio of internal radius to external radius of the rock ring is small enough ($\rho < 0.3$), specimens mostly split along the diametral loading line. With the increase of the ratio, the secondary cracks are formed in the direction perpendicular to the loading line. Under dynamic loading tests, specimens usually break up into four pieces. When the ratio ρ reaches 0.5, the secondary cracks are formed near the input bar. The tensile strength calculated by Hobbs' formula is greater than the Brazilian splitting strength. The peak load and the radius ratio show a negative exponential relationship under static test. Using ring specimen to determine tensile strength of rock material is more like a test indicator rather than the material properties.

Key words: rock; circular ring; Brazilian splitting test; tensile strength; split Hopkinson pressure bar; failure pattern

1 Introduction

The splitting test, also called the Brazilian test, is a simple and convenient method to obtain the indirect tensile strength of rock and rock-like materials. This method was firstly introduced by CARNEIRO [1] and AKAZAWA [2] in 1943. Over the past several decades, the Brazilian splitting test has received considerable attention. Although the splitting test was officially recommended by the International Society for Rock Mechanics (ISRM) as a method to determine the tensile strength of rock and rock-like materials in 1978 [3], the validity of the test has been always debated even until nowadays [4].

In 1965, the splitting test of a circular ring, disc with a small central hole, for determining the tensile strength of rock was proposed by HOBBS [5]. In his work, the distribution of the stress in a circular ring subjected to a splitting load was studied and a formula was provided to calculate the tensile strength. Since then,

the splitting test of a circular ring specimen to determine the indirect tensile strength of brittle material has received considerable attention. The distribution of stress and displacement in a circular ring under diametral compression has already been studied in the range of ρ values (the ratio of ring's radii) [6–8]. CHEN and HSU [9] studied the indirect tensile strength of anisotropic rock by the ring test through numerical methods. The results showed that the tensile strength of anisotropic rocks determined by ring test was not a constant, which depended on various factors. ZHU et al [10] and LIU et al [11] simultaneously considered the influence of ρ value on the tensile strength through numerical methods. The cracking load to determine the indirect tensile strength of rock was proposed [10] and the relation between the indirect tensile strength and the ρ value was obtained [11]. YOU et al [12] experimentally studied the influence of water condition on the tensile strength of rocks. It showed that the water condition could influence the tensile strength when the dimension of the internal hole reached a certain value and an

exponential equation was proposed to describe the relation between the maximum force and its internal diameter. Moreover, the ring test was proposed as a convenient method to determine the fracture toughness without pre-cracked specimens [13]. ZHANG and LIANG [14] calibrated the maximum dimensionless stress intensity factor for a holed flattened ring specimen.

The dynamic tensile strength of rocks is usually determined by the dynamic splitting test in split Hopkinson pressure bars (SHPB). ZHU et al [15,16] carried out the dynamic splitting test of disc specimen with SHPB driven by pendulum hammer, in order to determine the indirect tensile strength of rock under an intermediate strain rate. The strain rate dependency of tensile strength and the failure pattern of the Brazilian disc specimen under the intermediate strain rate were numerically simulated with RFPA-Dynamic. ZHOU et al [17,18] investigated the stress evolution and failure process of Brazilian disc with SHPB device. It was found that the stress distribution in specimen after equilibrium was similar to its static loading case, and the crack initiated at the disc center and propagated along the loading direction. DAI et al [19] used a SHPB system to quantify the dynamic tensile strength of rocks by the Brazilian disc (BD) specimen. It showed that with proper experimental design, the dynamic tensile strengths of rocks measured by using SHPB were valid and reliable. WANG et al [20,21] measured the dynamic tensile stress of rock by flattened Brazilian disc (FBD) specimens in a pulse shaping SHPB system, and drew a conclusion that the pattern of dynamic stress distribution in the specimen was symmetric and similar to that of the counterpart static loading. However, the dynamic ring test has not been reported in the available literatures.

In this work, the splitting test was used to investigate the static and dynamic properties of ring specimens for marble. The tensile strengths of the circular rock rings under static and dynamic loads were experimentally studied, and the failure patterns of the specimens under different loading rates were discussed.

2 Experimental

2.1 Specimen preparation

The specimens were firstly drilled from a single marble block with good geometrical integrity and petrographic uniformity. The cylindrical specimens were prepared with a diameter (D) of 50 mm and a length/diameter ratio (l/D) of 0.5. Then, most of the discs were taken to prepare circular ring specimens with internal diameters varying from 5 to 25 mm with an interval of 5 mm by water jet cutting technology. It means the ratio of internal radius to external radius of

rock ring (ρ) varies from 0.1 to 0.5 with an interval of 0.1.

The specimens were numbered after preparation. The number of the specimen reflected the testing method, the ratio of internal radius to external radius of rock ring and the sequence of preparing. Such as, S0.2-2 indicates that this specimen is the second specimen of the circular ring with an inner diameter of 10 mm and the ratio of 0.2, which is conducted under static compression. While D0-3 indicates that this specimen is the third one of the intact marble disc, which is conducted under dynamic impact test.

2.2 Test apparatus and scheme

The static tests were conducted on an Instron1342 system. Specimens were put directly between the platens. The displacement rate was set at 1.5 mm/min during the splitting test. The dynamic tests were performed on the SHPB system. The cylindrical elastic bars are made of steel with a density of 7.8 g/cm³, an elastic modulus of 240 GPa and a P-wave velocity of 5400 m/s. Dynamic loads came from the impact of a striker driven by high-pressure gas. Specimens were sandwiched between the incident bar and the transmitted bar during the test. The failure progress of the specimen was monitored by a high-speed camera (FASTCAM SA1.1). The tensile strength of the intact disc specimen was calculated by

$$\sigma_{t,S/D} = \frac{P}{\pi R t} \quad (1)$$

where $\sigma_{t,S}$ and $\sigma_{t,D}$ are tensile strengths under the static and dynamic loads, respectively; P is the maximum force applied on the specimen for the static test or the equivalent maximum force applied on the specimen for the dynamic one; R and t are the radius and the thickness of the specimen, respectively. The equivalent maximum force in the dynamic test can be obtained and calculated by [22]

$$P(t) = E A_e \varepsilon_T(t) \quad (2)$$

where E is the elastic modulus of the bar, A_e is the cross-sectional area of the bar, and $\varepsilon_T(t)$ is the transmitted pulse captured by the strain gauge on the transmitted bar.

According to Hobbs [5] equation, the formula for calculating the tensile strength σ_i^R in a circular ring is

$$\sigma_{i,S/D}^R = \frac{P}{\pi R t} \left(6 + 38 \frac{r^2}{R^2} \right) \quad (3)$$

where R and r are the external and internal radii, respectively; $\sigma_{i,S}^R$ represents the tensile strength under the static load and $\sigma_{i,D}^R$ represents the tensile strength under the dynamic load for rock ring specimens.

3 Results and discussion

3.1 Tensile strength and failure progress of Brazilian disc

The average static and dynamic tensile strengths of the marble were obtained as 3.60 MPa and 18.11MPa, respectively. Table 1 shows the basic physic-mechanical parameters and the static and dynamic tensile strengths of disc specimens. It can be found that the average dynamic tensile strength is about five times the static one for marble disc.

Table 1 Testing results of disc specimens

Specimen	Diameter/mm	Thickness/mm	Tensile strength/MPa
S0-1	49.95	25.94	2.72
S0-2	49.84	25.06	3.40
S0-3	49.91	24.88	4.68
Average	49.90	25.29	3.60
Specimen	Diameter/mm	Thickness/mm	Tensile strength/MPa
D0-1	49.86	25.07	17.10
D0-2	49.72	24.86	24.40
D0-3	49.86	25.07	12.83
Average	49.81	25.00	18.11

Figure 1 shows the failure mode and progress of typical disc specimen under static and dynamic loads. As shown in Fig. 1, the failure progress of the two discs can be classified into five periods. With the increase of load, there are some white patches appearing along the loading line, where the tensile stress reaches the tensile strength of the rock. Finally, both of two discs are split into two semicircular fragments.

3.2 Tensile strength of ring specimen

3.2.1 Static tensile strength

Testing results of ring specimens under static loads

are shown in Table 2. It can be seen that the maximum force of circular ring decreases with the increase of the internal diameter. Figure 2 shows the relationship between the peak force and the ratio of ρ . The average peak force decreases exponentially with the increase of ρ value.

Table 2 Physic-mechanical parameters and peak force of circular ring specimens under static loads

Specimen	External diameter, D/mm	Internal diameter, d/mm	Thickness, t/mm	Peak force, P/kN	Average Failure P/kN	Failure mode
S0.1-1	49.74	5.84	24.98	5.62		I
S0.1-2	49.76	5.92	25.31	5.43	5.51	I
S0.1-3	49.77	5.82	25.12	5.47		I
S0.2-1	49.83	10.81	24.97	4.02		I
S0.2-2	49.82	10.69	24.54	4.24	4.13	II
S0.2-3	49.85	10.77	25.08	4.14		I
S0.3-1	49.76	15.49	26.24	2.73		II
S0.3-2	49.79	15.53	24.89	2.70	2.70	II
S0.3-3	49.55	15.39	25.03	2.66		II
S0.4-1	49.82	20.67	23.76	1.59		II
S0.4-2	49.63	20.15	25.35	1.79	1.71	II
S0.4-3	49.83	20.36	25.32	1.75		II
S0.5-1	49.76	25.74	26.70	0.96		II
S0.5-2	49.85	25.76	24.75	0.82	0.90	II
S0.5-3	49.85	25.64	24.72	0.92		II

Figure 3 shows the typical force–time curves of specimens under static loads with different internal diameters. It can be seen from the force–time curves that the curves are obviously different from each other. The force–time curves of the circular rings with small internal diameters have two peaks before the breakage of specimens, then the curves drop rapidly. However, the curves of circular ring with large internal diameters have

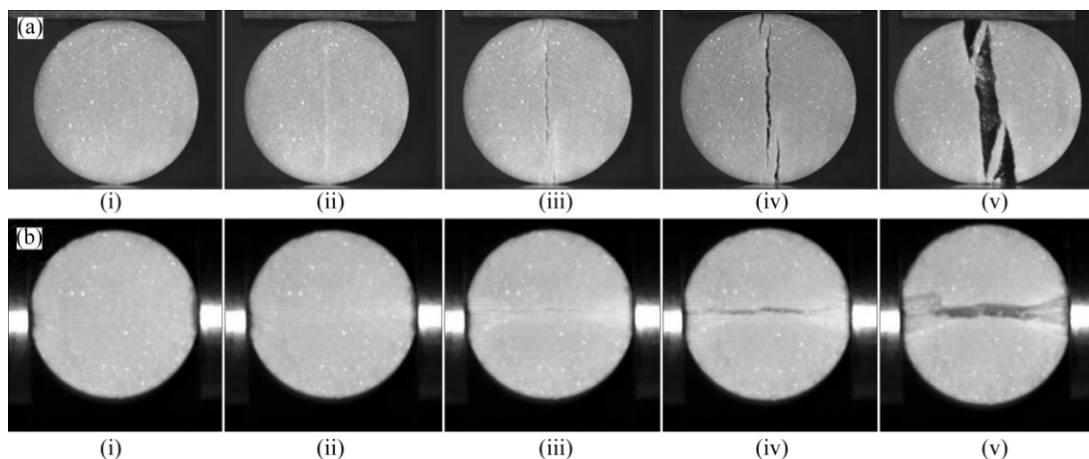


Fig. 1 Failure progress of Brazilian discs under static (a) and dynamic (b) loads: (i) Loading contact of specimen; (ii) White patches appearing; (iii) Initial fracture; (iv) Macro fracture appearing; (v) Final failure mode

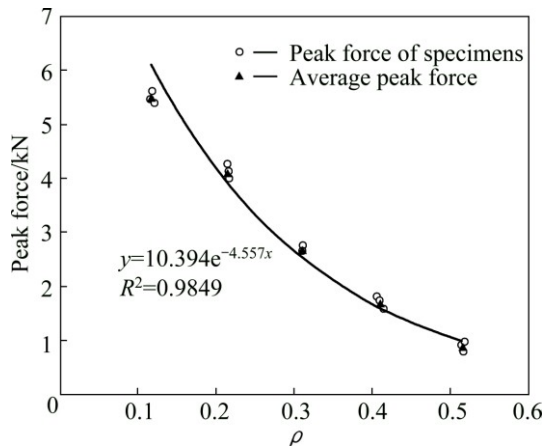


Fig. 2 Relationship between static peak force and ρ value

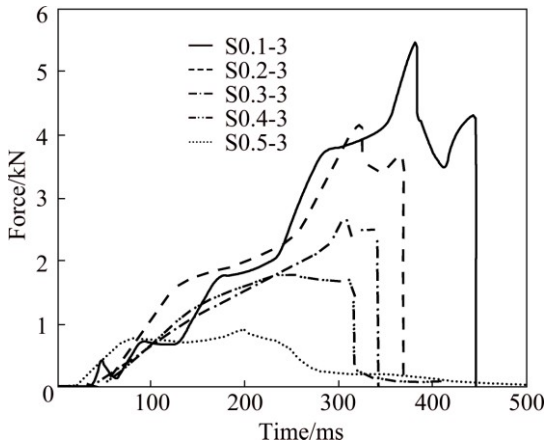


Fig. 3 Force–time curves of circular ring specimens under static loads

a flat period before the breakage, and the curves cannot reach the coordinate axis when the samples have breakage due to the configuration of the devices.

The static tensile strengths calculated by Eq. (3) are listed in Table 3. Compared with the Brazilian tensile strength, the calculated tensile strengths of circular ring specimens overestimate this material property. The ratio of $\sigma_{t,S}^R/\sigma_{t,S}$ varies from 5.08 to 2.03 when ρ increases from 0.1 to 0.5.

Table 3 Calculated static tensile strengths of circular ring specimens

ρ	0.1	0.2	0.3	0.4	0.5
$\sigma_{t,D}^R/\text{MPa}$	18.30	16.51	13.17	10.91	7.30

3.2.2 Dynamic tensile strength

The stress waves, particularly the transmitted stress waves of the ring specimens, are obviously influenced by the dimension of the internal hole. With the increase of the internal diameter, the transmitted wave becomes almost a flat linear line. Figure 4 shows the comparison

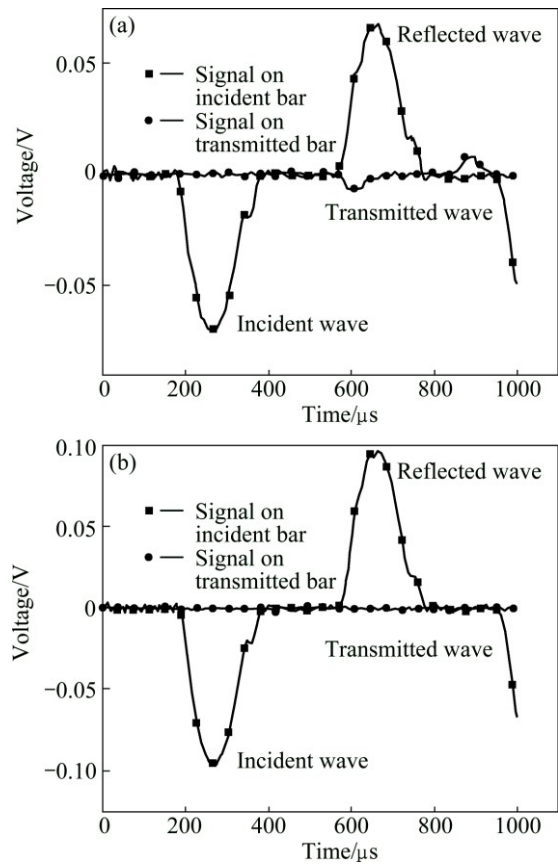


Fig. 4 Typical original electrical pulse signals of ring specimens under dynamic tests: (a) Specimen D0.1-3; (b) Specimen D0.5-2

of original electrical pulse signals of two typical ring specimens. It means that for the ring specimen with a large internal diameter, most of the incident stress is reflected to the incident bar and only a very little part is transmitted to the transmitted bar. The failure of the large internal diameter ring specimens needs much less energy compared with the small internal hole ring specimens.

Testing results of ring specimens under dynamic loads are shown in Table 4. The calculated tensile strength $\sigma_{t,D}^R$ is affected by the dimension of the internal hole and decreases with the increase of the internal diameter. The $\sigma_{t,D}^R/\sigma_{t,D}$ ratio varies from 5.28 to 2.08.

Theoretically, when the maximum tensile stress reaches the tensile strength of the marble, the tensile fracture will initiate from the surface of the internal hole along the diametral loading line in the ring specimen. However, the ring specimen still has loading capacity before the final failure of the specimen and the calculated tensile stress may still increase with the increase of the loads. Therefore, the tensile strength calculated by Eq. (3) using the maximum load or transmitted pulse may lead to a higher value than that using the fracture initiation load or pulse.

Table 4 Physic-mechanical parameters and $\sigma_{t,D}^R$ of circular ring specimens under dynamic loads

Specimen	External diameter, D/mm	Internal diameter, d/mm	Thickness, t/mm	$\sigma_{t,D}^R/\text{MPa}$	Average $\sigma_{t,D}^R/\text{MPa}$	Failure mode
D0.1-1	49.76	5.89	25.80	–		–
D0.1-2	49.69	5.99	25.78	80.94	95.69	A
D0.1-3	49.71	5.99	25.84	110.44		A
D0.2-1	49.67	10.49	25.70	98.63		A
D0.2-2	49.71	10.53	25.83	93.62	94.27	A
D0.2-3	49.73	10.43	26.15	90.56		A
D0.3-1	49.73	15.33	25.83	75.69		A
D0.3-2	49.60	15.51	25.59	82.63	79.92	A
D0.3-3	49.68	15.62	25.63	81.44		A
D0.4-1	49.74	19.81	25.75	79.12		A
D0.4-2	49.67	20.16	25.84	94.24	80.56	A
D0.4-3	49.76	20.29	25.92	68.33		A
D0.5-1	49.72	25.13	25.64	39.85		B
D0.5-2	49.74	25.16	25.78	46.96	37.67	B
D0.5-3	49.71	24.96	25.64	26.21		A

3.3 Failure modes of ring specimens

The failure modes of ring specimens play an important role in revealing the failure mechanism of rocks under diametrical splitting test. By using high-speed camera technology, the fracture mode of the circular ring specimen can be easily identified.

Two types of failure modes are found by collecting and checking the broken rock pieces after static tests. Type I is a diametrical splitting. In the previous researches, the traveling direction of the crack from the internal to the external diameter was found and established [5]. The specimen with a lower ρ value ($\rho < 0.3$) is usually split into two fragments, which are similar with the final failure modes of Brazilian discs. Type II is a four-fun-shaped failure. Besides the cracks along the loading diameter, there are secondary cracks formed in each half ring. Most of the specimens with a higher ρ value ($\rho > 0.3$) belong to this type. When the crack along the loading diameter propagates, the load falls. Then, the load is supported by the two half rings, and the stress in the two halves could reach the tensile strength of the material, similar as the stress in a curved beam. Finally, the secondary cracks are formed in each half disk as shown in Fig. 5(b). Figure 6 shows the typical failure modes of ring specimen with different internal diameters.

In the dynamic tests, two types of failure modes were also found by analyzing the high speed images of ring specimens. Type A is a symmetrical four-fan-shaped ring. Type B is an asymmetrical four-fan-shaped ring. The two types of specimens break into four-fan-shaped rings. The secondary cracks are observed perpendicular

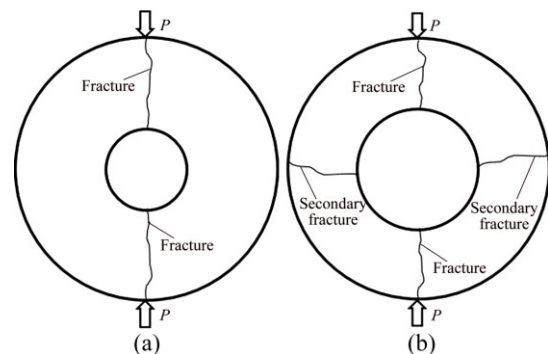


Fig. 5 Failure modes of specimens under static load: (a) Type I, diametrical split; (b) Type II, four-fan-shaped failure

to the loading diameter in the specimen of the Type A, while the cracks are observed approaching the incident bar in the specimen of Type B, as shown in Fig. 7. Meanwhile, it can be seen in Fig. 8 that with the increase of the ratio ρ , the final failure fractures become simpler and less. Moreover, with the increase of the internal diameter, the secondary tensile cracks will initiate near the incident bar. This indicates that the stress balance may be difficult to be achieved when the internal diameter increases to a certain value. Under this condition, the dynamic ring test under load will show more structural response instead of impact experimental or material response.

4 Conclusions

1) Experimental analyses have shown that the calculated tensile strength decreases with the increase of

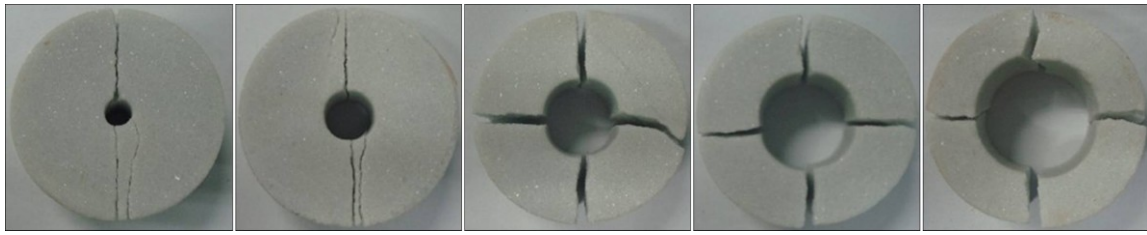


Fig. 6 Final failure modes of specimens under static loads (loading direction: vertical)

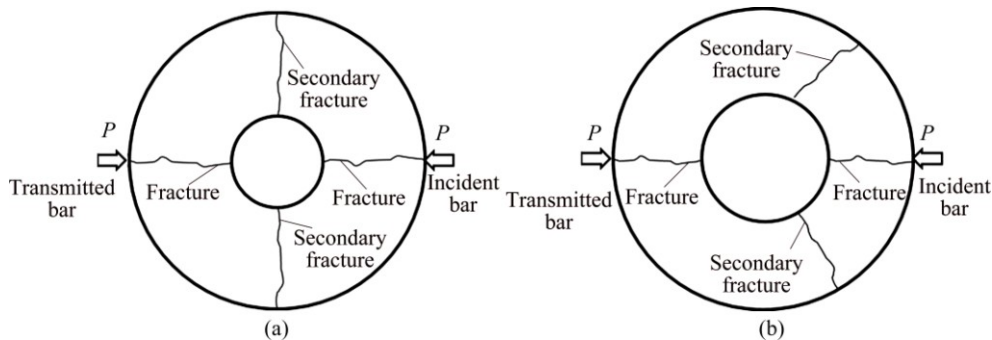


Fig. 7 Failure modes of specimens under dynamic load: (a) Type A, symmetrical failure; (b) Type B, asymmetrical failure

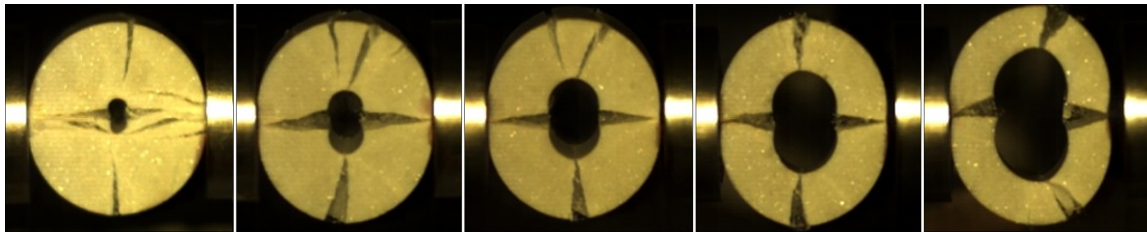


Fig. 8 Final failure modes of specimens under dynamic loads (Loading direction: horizontal)

ρ value. Otherwise, the strength calculated by Eq. (3) overestimates the tensile strength, compared with the tensile strength by the Brazilian splitting test. The ratio of the two strengths σ_t^R/σ_t varies from 5.08 to 2.03 for static tests and from 5.28 to 2.08 for dynamic tests. The test results indicate that the tensile strength obtained by ring test may be an experimental property rather than a material property.

2) Specimens with different internal radii have different failure patterns. For static splitting test, when $\rho < 0.3$, the ring specimen cracks are similar as those of the disc specimen under static splitting load. When $\rho > 0.3$, there are secondary cracks initiating in the specimens because the stress in the ring specimens has been changed. For dynamic splitting test, the secondary cracks can be found in each specimen. However, when $\rho = 0.5$, the cracks initiate near the incident bar, while others initiate at the line perpendicular to the loading line.

References

- [1] CARNEIRO F. A new method to determine the tensile strength of concrete [C]//Proceedings of the 5th Meeting of the Brazilian Association for Technical Rules. Rio de Janeiro, 1943: 126–129. (in Portuguese)
- [2] AKAZAWA T. New test method for evaluating internal stress due to compression of concrete: The splitting tension test [J]. J Japan Soc Civil Eng, 1943, 29: 777–787. (in Japanese)
- [3] International Society for Rock Mechanics. Suggested methods for determining tensile strength of rock materials [J]. International Journal of Rock Mechanics & Mining Science & Geomechanics Abstracts, 1978, 15(15): 99–103.
- [4] LI D Y, WONG L N Y. The Brazilian disc test for rock mechanics applications: Review and new insights [J]. Rock Mechanics & Rock Engineering, 2013, 46(2): 269–287.
- [5] HOBBS D W. An assessment of a technique for determining the tensile strength of rock [J]. British Journal of Applied Physics, 1965, 16(2): 259–268.
- [6] TOKOVYY Y V, HUNG K M, MA C C. Determination of stresses and displacements in a thin annular disk subjected to diametral compression [J]. Journal of Mathematical Sciences, 2010, 165(3): 342–354.
- [7] KOURKOULIS S K, MARKIDES C F. Stresses and displacements in a circular ring under parabolic diametral compression [J]. International Journal of Rock Mechanics & Mining Sciences, 2014, 71: 272–292.
- [8] MELLOR M, HAWKES I. Measurement of tensile strength by diametral compression of discs and annuli [J]. Engineering Geology, 1971, 5(3): 173–225.

- [9] CHEN C S, HSU S C. Measurement of indirect tensile strength of anisotropic rocks by the ring test [J]. *Rock Mechanics & Rock Engineering*, 2001, 34(4): 293–321.
- [10] ZHU Wan-cheng, FENG Dan, ZHOU Jin-tian, TANG Chun-an. Numerical test using ring specimen as medium to determine indirect tensile strength of rock [J]. *Journal of Northeastern University: Natural Science*, 2004, 25(9): 899–902. (in Chinese)
- [11] LIU Wen-bin, TANG Chun-an, ZHANG Hou-quan. Influence of internal radius of ring specimen on tensile strength of rock [J]. *Geotechnical Engineering Technique*, 2005, 18(6): 286–290. (in Chinese)
- [12] YOU Ming-qing, CHEN Xiang-lei, SU Cheng-dong. Brazilian splitting strengths of discs and rings of rock in dry and saturated conditions [J]. *Chinese Journal of Rock Mechanics and Engineering*, 2011, 30(3): 464–472. (in Chinese)
- [13] STAROSELSKY A. The express method of determining the fracture toughness of brittle materials [J]. *International Journal of Fracture*, 1999, 98(3): 47–52.
- [14] ZHANG Sheng, LIANG Ya-lei. Calibration of three-dimensional maximum dimensionless stress intensity factor of holed flattened Brazilian disc specimen [J]. *The Chinese Journal of Nonferrous Metals*, 2012, 22(8): 2347–2352. (in Chinese)
- [15] ZHU W C, NIU L L, LI S H, XU Z H. Dynamic Brazilian test of rock under intermediate strain rate: Pendulum hammer-driven SHPB test and numerical simulation [J]. *Rock Mechanics & Rock Engineering*, 2015, 48(5): 1–15.
- [16] ZHU W C, TANG C A. Numerical simulation of Brazilian disk rock failure under static and dynamic loading [J]. *International Journal of Rock Mechanics & Mining Sciences*, 2006, 43(2): 236–252.
- [17] ZHOU Z L, LI X B, ZOU Y, JIANG Y H, LI G N. Dynamic Brazilian tests of granite under coupled static and dynamic loads [J]. *Rock Mechanics & Rock Engineering*, 2014, 47(2): 495–505.
- [18] ZHOU Z L, ZOU Y, LI X B, JIANG Y H. Stress evolution and failure process of Brazilian disc under impact [J]. *Journal of Central South University*, 2013, 20(1): 172–177.
- [19] DAI F, HUANG S, XIA K, TAN Z. Some fundamental issues in dynamic compression and tension tests of rocks using split Hopkinson pressure bar [J]. *Rock Mechanics and Rock Engineering*, 2010, 43(6): 657–666.
- [20] WANG Q Z, LI W, XIE H P. Dynamic split tensile test of flattened Brazilian disc of rock with SHPB setup [J]. *Mechanics of Materials*, 2009, 41(3): 252–260.
- [21] WANG Q Z, ZHANG S, XIE H P. Rock dynamic fracture toughness tested with holed-cracked flattened Brazilian discs diametrically impacted by SHPB and its size effect [J]. *Experimental Mechanics*, 2010, 50(7): 877–885.
- [22] LI Xi-bin. *Rock dynamics fundamentals and applications* [M]. Beijing: Science Press, 2014. (in Chinese)

基于圆环劈裂试验的岩石静态和动态拉伸破坏特性

李地元¹, 王涛¹, 成腾蛟², 孙小磊¹

1. 中南大学 资源与安全工程学院, 长沙 410083;

2. 中国瑞林工程技术有限公司, 南昌 330031

摘要: 对不同内径的大理岩圆环试样进行静态和动态劈裂试验, 研究其在不同加载速率下的抗拉强度和破坏模式随内外径比值(ρ)的变化规律。结果表明: 圆盘试样的动态抗拉强度约为其静态抗拉强度的 5 倍。圆环试样的破坏模式与试样内径大小以及加载速率有关。在静载试验条件下, 当试样内外径比较小($\rho < 0.3$)时, 试样以沿加载径向劈裂破坏为主, 而随着内外径比的增大, 在垂直加载方向上产生次生拉伸裂纹。在冲击荷载作用下, 圆环破裂成 4 块, 且当试样内外径比为 0.5 时, 次生裂纹靠近入射杆。采用 Hobbs 公式计算的抗拉强度均比巴西圆盘的劈裂强度大, 且静态劈裂试验的峰值荷载和圆环试样的内外径比呈负指数变化规律。利用圆环试样确定的岩石抗拉强度更像是材料的一种试验指标而不是材料属性。

关键词: 岩石; 圆环; 巴西劈裂试验; 抗拉强度; 分离式霍普金森压杆; 破坏模式

(Edited by Wei-ping CHEN)